

Quantum algorithm for simulating real time evolution of lattice Hamiltonians

Jeongwan Haah,¹ Matthew B. Hastings,^{1,2} Robin Kothari,¹ and Guang Hao Low¹

¹*Quantum Architectures and Computation,*

Microsoft Research, Redmond, Washington, USA

²*Station Q, Microsoft Research, Santa Barbara, California, USA*

We present a decomposition of the real time evolution operator e^{-iTH} of any local Hamiltonian H on lattices $\Lambda \subseteq \mathbb{Z}^D$ into local unitaries based on Lieb-Robinson bounds. Combining this with recent quantum simulation algorithms for real time evolution, we find that the resulting quantum simulation algorithm has gate count $\mathcal{O}(Tn \text{polylog}(Tn/\epsilon))$ and depth $\mathcal{O}(T \text{polylog}(Tn/\epsilon))$, where n is the space volume or the number of qubits, T is the time of evolution, and ϵ is the accuracy of the simulation in operator norm. In contrast to this, the previous best quantum algorithms have gate count $\mathcal{O}(Tn^2 \text{polylog}(Tn/\epsilon))$. Our approach readily generalizes to time-dependent Hamiltonians as well, and yields an algorithm with similar gate count for any piecewise slowly varying time-dependent bounded local Hamiltonian. Finally, we also prove a matching lower bound on the gate count of such a simulation, showing that any quantum algorithm that can simulate a piecewise time-independent bounded local Hamiltonian in one dimension requires $\tilde{\Omega}(Tn)$ gates in the worst case. In the appendix, we prove a Lieb-Robinson bound tailored to Hamiltonians with small commutators between local terms. Unlike previous Lieb-Robinson bounds, our version gives zero Lieb-Robinson velocity in the limit of commuting Hamiltonians. This improves the performance of our algorithm when the Hamiltonian is close to commuting.

I. INTRODUCTION

A Hamiltonian is a Hermitian operator H on a Hilbert space that generates the unitary dynamics U_t^H of a system of interacting degrees of freedom by the Schrödinger equation $i\partial_t U_t^H = HU_t^H$. It is standard that any physical system can be modeled by a *local* Hamiltonian,¹ meaning H is a sum of terms, each of which is supported on a ball of small diameter (interaction range) with respect to the natural metric of the space the system lives in. Regarding Nature as a quantum simulator, one expects that the gate complexity of the real time evolution operator should be linear in the spacetime volume. However, so far quantum algorithms that simulate real time evolution do not achieve this linear scaling, even for a one-dimensional Hamiltonian with nearest-neighbor interactions [2].

¹ Confusingly, this term is used to describe two different kinds of Hamiltonians in the literature. In this paper we use the term *local* to refer to geometrically local Hamiltonians as defined above. In the other usage, a k -local Hamiltonian is a Hamiltonian that is the sum of terms which each act nontrivially on k particles without any reference to their geometry (see, e.g., [1]).

This is largely because the best known algorithms for sparse Hamiltonian simulation [3–5] work just as well for geometrically non-local Hamiltonians and are not tailored to local Hamiltonians. And intuitive Lie-Trotter-Suzuki expansions [6, 7] might achieve linear scaling, and indeed they appear to do so empirically [2], but we do not understand well how to analyze the error in the expansion. Here we discuss Hamiltonians on a lattice of qubits and call the readers’ attention to a decomposition of the time evolution unitary based on Lieb-Robinson bounds [8–12], that is made explicit by Osborne [13] (see also Michalakis [14, Sec. III]), which when combined with recent advances [3–5], gives an algorithm with gate complexity matching Nature’s, up to logarithmic factors. Osborne phrased his results in terms of classical simulation of one-dimensional quantum chains, but adaptation to quantum simulation is transparent. We simplify the “patching” unitaries in [13, 14] by going through the “interaction picture,” and, in consequence, make generalizations to higher dimensions easy.

Our normalization convention and assumptions are as follows. Let $H = \sum_{X \subseteq \Lambda} h_X$ be a *local* Hamiltonian on a finite lattice $\Lambda \subseteq \mathbb{Z}^D$ such that $\|h_X\| \leq 1$ for every X . Each term may or may not depend on time. Here locality means that h_X is supported on region X , and $h_X = 0$ whenever $\text{diam}(X) > 1$. We assume that there are $\mathcal{O}(1)$ qubits per lattice site. These conditions are not restrictions at all since we can rescale the spacetime metric for the norm bound and the locality to hold. More physically speaking, the distance and the norm of Hamiltonian (energy) are not dimensionless quantities, and we set our units for these properties to hold. The space dimension D is considered constant, and hence it is ignored in asymptotic expressions using big- \mathcal{O} notation.

For any subset $S \subseteq \Lambda$ of sites, we denote by H_S the sum $\sum_{X \subseteq S} h_X$; hence, $H_\Lambda = H$. For any subset S of sites, let $|S|$ denote the number of sites in S .

We say that a function $\alpha : [0, 1] \ni t \mapsto \alpha(t) \in \mathbb{R}$ is **efficiently computable** if there is an algorithm that outputs $\alpha(t)$ to precision ϵ for any given input t specified to precision ϵ in running time $\text{polylog}(1/\epsilon)$. Note that any complex-valued analytic function on a nonzero neighborhood of a closed interval in the complex plane is efficiently computable. See [Appendix B](#). We say that a function α on the interval $[0, T]$ ($T \geq 1$) is **piecewise slowly varying** if there are $M = \mathcal{O}(T)$ intervals $[t_{j-1}, t_j]$ with $0 = t_0 < t_1 < \dots < t_M = T$ such that $\partial_t \alpha(t)$ exists and is bounded by $1/(t_j - t_{j-1})$ for $t \in (t_{j-1}, t_j)$.

A function whose domain is an interval of length $T \geq 1$ is said to be efficiently computable if there are $\mathcal{O}(T)$ slices of length ≤ 1 of the domain, in each of which the function is efficiently computable. We say an operator $h(t)$ is efficiently computable, if it can be written as $h(t) = \sum_j \alpha_j(t) P_j$ where P_j are tensor products of Pauli matrices, and every $\alpha_j(t) \in \mathbb{R}$ is efficiently computable. Likewise,

an operator $h(t)$ is said to be piecewise slowly varying if every $\alpha_j(t)$ is piecewise slowly varying with respect to a time slicing independent of j .

II. ALGORITHM AND ANALYSIS

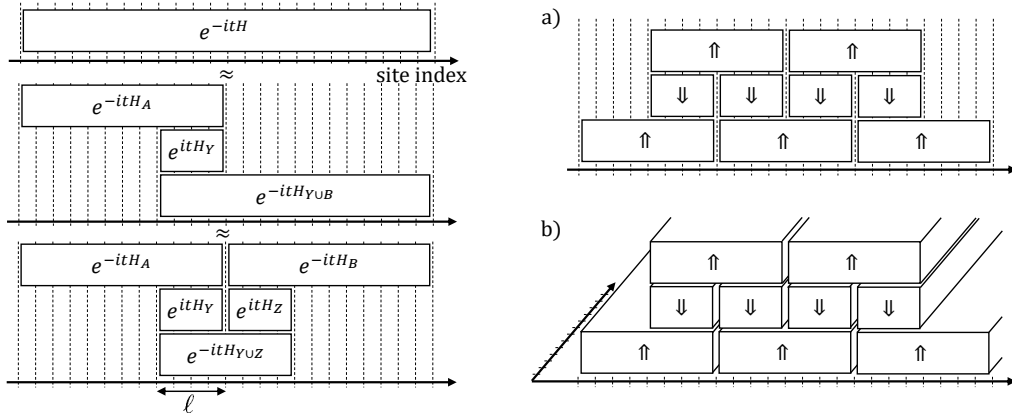


FIG. 1. Decomposition of time evolution operator for time $t = \mathcal{O}(1)$. The time is going upwards. Each block \square represents the forward time evolution, e^{-itH_\square} , if the arrow is upward, and backward time evolution, e^{+itH_\square} , if the arrow is downward. Here, H_\square is the sum of local terms in the Hamiltonian supported within the block. The overlap has size ℓ . (a) shows a one-dimensional setting, but a generalization to higher D dimensions is readily achieved by regarding each block as a $(D-1)$ -dimensional hyperplane so that the problem reduces to lower dimensions. (b) shows a two-dimensional setting. The approximation error from the depicted decomposition is $\epsilon = \mathcal{O}(e^{-\mu\ell} L^D / \ell)$ where L is the linear system size, ℓ is the width of the overlap between blocks, and $\mu > 0$ is a constant that depends only on the locality of the Hamiltonian. One can use any algorithm to further decompose the resulting “small” unitaries on $\mathcal{O}(\log(L/\epsilon))$ qubits into elementary gates. To achieve gate count that is linear (up to logarithmic factors) in spacetime volume, the algorithm for simulating the blocks needs to be polynomial in the block size and polylogarithmic in accuracy.

Theorem 1. *Let $H = \sum_{X \subseteq \Lambda} h_X(t)$ be a time-dependent Hamiltonian on a lattice Λ of n qubits, embedded in the Euclidean metric space \mathbb{R}^D . Assume that every unit ball contains $\mathcal{O}(1)$ qubits, $h_X = 0$ if $\text{diam}(X) > 1$. Also assume that every local term $h_X(t)$ is efficiently computable (e.g., analytic), piecewise slowly varying on time domain $[0, T]$, and $\|h_X(t)\| \leq 1$ and for any X and t . Then, there exists a quantum algorithm that can approximate the real-time evolution of H for time T to accuracy ϵ using $\mathcal{O}(Tn \text{polylog}(Tn/\epsilon))$ 2-qubit local gates, and has depth $\mathcal{O}(T \text{polylog}(Tn/\epsilon))$.*

The algorithm is depicted in Figure 1. Before showing why this algorithm works, we provide a high-level overview of the algorithm and the structure of the proof. Since a time evolution unitary

$U(T; 0)$ is equal to $U(T = t_M; t_{M-1})U(t_{M-1}, t_{M-2}) \cdots U(t_2; t_1)U(t_1; t_0 = 0)$, we will focus on a time evolution operator $U(t; 0)$ where $t = (\infty)$, generated by a slowly varying bounded Hamiltonian. The key idea, as shown in [Figure 1](#), is that the time-evolution operator, e^{-itH} due to the full Hamiltonian $\sum_{X \subseteq \Lambda} h_X$ can be approximately written as a product $e^{-itH_A}e^{+itH_Y}e^{-itH_{Y \cup B}}$. Here $A \cup B = \Lambda$ and we think of A and B as large regions, but Y as a small subset of A . The error in the approximation is exponentially small as long as Y is large enough. This is formally proved in [Lemma 4](#), which is supported by [Lemma 2](#) and [Lemma 3](#). Applying this twice leads to a symmetric approximation as depicted at the bottom left of [Figure 1](#). This procedure can then be repeated for the large operators supported on A and B to reduce the size of all the operators involved, leading to the pattern in [Figure 1](#) (a). This reduces the problem of implementing the time-evolution operator for H into the problem of implementing smaller time-evolution operators, which can be implemented using known quantum algorithms.

We now establish the lemmas needed to prove the result.

Lemma 2. *Let A_t and B_t be continuous time-dependent Hermitian operators, and let U_t^A and U_t^B with $U_0^A = U_0^B = \mathbf{1}$ be the corresponding time evolution unitaries. Then the following hold:*

- (i.) *$W_t = (U_t^B)^\dagger U_t^A$ is the unique solution of $i\partial_t W_t = ((U_t^B)^\dagger (A_t - B_t)U_t^B) W_t$ and $W_0 = \mathbf{1}$.*
- (ii.) *If $\|A_s - B_s\| \leq \delta$ for all $s \in [0, t]$, then $\|U_t^A - U_t^B\| \leq t\delta$.*

Proof. (i) Differentiate. The solution to the ordinary differential equation is unique. (ii) Apply Jensen's inequality for $\|\cdot\|$ (implied by the triangle inequality for $\|\cdot\|$) to the equation $W_t - W_0 = \int_0^t ds \partial_s W_s$. Then, invoke (i) and the unitary invariance of $\|\cdot\|$. \square

Lemma 3 (Lieb-Robinson bound [\[8–11\]](#)). *Let $H = \sum_X h_X$ be a local Hamiltonian and O_X be any operator supported on X , and put $\ell = \lfloor \text{dist}(X, \Lambda \setminus \Omega) \rfloor$. Then*

$$\left\| (U_t^H)^\dagger O_X U_t^H - (U_t^{H_\Omega})^\dagger O_X U_t^{H_\Omega} \right\| \leq |X| \|O_X\| \frac{(2\zeta_0|t|)^\ell}{\ell!} e^{2\zeta_0|t|}, \quad (1)$$

where $\zeta_0 = \max_{p \in \Lambda} \sum_{Z \ni p} |Z| \|h_Z\| = \mathcal{O}(1)$. In particular, there are constants $v_{LR} > 0$, called the Lieb-Robinson velocity, and $\mu > 0$, such that for $\ell \geq v_{LR}|t|$, we have

$$\left\| (U_t^H)^\dagger O_X U_t^H - (U_t^{H_\Omega})^\dagger O_X U_t^{H_\Omega} \right\| \leq \mathcal{O}(|X| \|O_X\| \exp(-\mu\ell)). \quad (2)$$

Proof. See [Appendix A 4](#). \square

We are considering strictly local interactions (as in [Theorem 1](#)), where $h_X = 0$ if $\text{diam}(X) > 1$, but similar results hold with milder locality conditions such as $\|h_X\| \leq e^{-\text{diam}(X)}$ [\[8–12\]](#); see the appendix for a detailed proof. Below we will only use the result that the error is at most $\mathcal{O}(e^{-\mu\ell})$ for some $\mu > 0$ and fixed t . For slower decaying interactions, the bound is weaker and the overlap size ℓ in [Figure 1](#) will have to be larger.

The Lieb-Robinson bound implies the following decomposition.

Lemma 4. *Let $H = \sum_X h_X$ be a local Hamiltonian (as in [Theorem 1](#), or a more general definition for which [Lemma 3](#) still holds). Then there are constants $v, \mu > 0$ such that for any disjoint regions A, B, C , we have*

$$\left\| U_t^{H_{A \cup B}} (U_t^{H_B})^\dagger U_t^{H_{B \cup C}} - U_t^{H_{A \cup B \cup C}} \right\| \leq \mathcal{O}(e^{vt - \mu \text{dist}(A, C)}) \sum_{X: \text{bd}(AB, C)} \|h_X\| \quad (3)$$

where $X : \text{bd}(AB, C)$ means that $X \subseteq A \cup B \cup C$ and $X \not\subseteq A \cup B$ and $X \not\subseteq C$.

Proof. We omit “ \cup ” for the union of disjoint sets. The following identity is trivial but important:

$$U_t^{H_{ABC}} = U_t^{H_{AB} + H_C} \underbrace{(U_t^{H_{AB} + H_C})^\dagger U_t^{H_{ABC}}}_{=W_t}. \quad (4)$$

By [Lemma 2](#) (i), W_t is generated by [\[13, 14\]](#)

$$\begin{aligned} & (U_t^{H_{AB} + H_C})^\dagger \underbrace{(H_{ABC} - H_{AB} - H_C)}_{H_{\text{bd}}} U_t^{H_{AB} + H_C} \\ &= (U_t^{H_B + H_C})^\dagger H_{\text{bd}} U_t^{H_B + H_C} + \underbrace{\mathcal{O}(\|H_{\text{bd}}\| e^{vt - \mu\ell})}_{=\delta} \end{aligned} \quad (5)$$

where ℓ is the distance from the support of the boundary terms H_{bd} to A , and the estimate of δ is due to [Lemma 3](#) applied to local terms in H_{bd} . Since H_{bd} contains terms that cross between AB and C , the distance ℓ is at least $\text{dist}(A, C)$ minus 2. By [Lemma 2](#) (i) again, the unitary generated by the first term of (5) is $(U_t^{H_B + H_C})^\dagger U_t^{H_{BC}}$, which can be thought of as the “interaction picture” time-evolution operator of the Hamiltonian in (5). This is our simplification of the “patching” unitary, which is $t\delta$ -close to W_t by [Lemma 2](#) (ii). \square

The decomposition of time evolution unitary in [Figure 1](#) is a result of iterated application of [Lemma 4](#). For a one-dimensional chain, let L be the length of the chain, so there are $\mathcal{O}(L)$ qubits. Take a two contiguous blocks Y and Z of the chain that overlaps by length $\ell \ll L$. Under periodic boundary conditions there are two components in the intersection, and under open boundary conditions, there is one component in the intersection. Applying [Lemma 4](#), we decompose the

full unitary into two blocks on Y and Z , respectively, and one or two blocks in the intersection. Every block unitary in the decomposition is a time evolution operator with respect to the sum of Hamiltonian terms within the block, and we can recursively apply the decomposition. Making the final blocks as small as possible, we end up with a layout of small unitaries as shown in Figure 1 (a). The error from this decomposition is $\mathcal{O}(\delta L/\ell)$, which is exponentially small in ℓ for $t = \mathcal{O}(1)$.

Going to higher dimensions $D > 1$, we first decompose the full time evolution into unitaries on $\mathcal{O}(L/\ell)$ hyperplanes (codimension 1). This entails error $\mathcal{O}(e^{-\mu\ell} L^D/\ell)$ since the boundary term has norm at most $\mathcal{O}(L^{D-1})$. For each hyperplane the decomposition into $\mathcal{O}(L/\ell)$ blocks of codimension 2 gives error $\mathcal{O}(e^{-\mu\ell} (\ell L^{D-2})(L/\ell))$. Summing up all the hyperplanes, we get $\mathcal{O}(e^{-\mu\ell} L^D/\ell)$ for the second round of decomposition. After D rounds of the decomposition the total error is $\mathcal{O}(e^{-\mu\ell} D L^D/\ell)$, and we are left with $\mathcal{O}((L/\ell)^D)$ blocks of unitaries for $t = \mathcal{O}(1)$. For longer times, apply the decomposition to each factor of $U(T = t_M; t_{M-1})U(t_{M-1}, t_{M-2}) \cdots U(t_2; t_1)U(t_1; t_0 = 0)$.

It remains to implement the unitaries on $m = \mathcal{O}(TL^D/\ell^D)$ blocks \square of $\mathcal{O}(\ell^D)$ qubits where $\ell = \mathcal{O}(\log(TL/\epsilon))$ to accuracy ϵ/m . All blocks have the form $U_t^{H\square}$, and can be implemented using any known Hamiltonian simulation algorithm. For a time-independent Hamiltonian, if we use an algorithm that is polynomial in the spacetime volume and polylogarithmic in the accuracy such as those based on signal processing [4, 5] or linear combination of unitaries [3, 15, 16], then the overall gate complexity is $\mathcal{O}(TL^D \text{polylog}(TL/\epsilon)) = \mathcal{O}(Tn \text{polylog}(Tn/\epsilon))$, where the exponent in the polylog factor depends on the choice of the algorithm. For a slowly varying time-dependent Hamiltonian, we can use the fractional queries algorithm [15] or the Taylor series approach [3] to achieve the same gate complexity. The Taylor series approach uses a subroutine $|t\rangle \mapsto |t\rangle \left(\sum_j |\alpha_j(t)| \right)^{-1/2} \sum_j \sqrt{\alpha_j(t)} |j\rangle$, where $\alpha_j(t)$ is the real coefficient of Pauli operator P_j in the Hamiltonian, which must be efficiently evaluated. For not too large system sizes L , it may be reasonable to use a bruteforce method to decompose the block unitaries into elementary gates [17, Chap. 8].

We have completed the proof of Theorem 1.

III. INHOMOGENEOUS INTERACTION STRENGTH

We can adapt the decomposition of the time-evolution unitary based on Lieb-Robinson bounds when there is inhomogeneity in interaction strength across the lattice. For this section, we do not assume that $\|h_X\| \leq 1$ for all $X \subseteq \Lambda$. Instead, suppose there is one term h_{X_0} in the Hamiltonian with $\|h_{X_0}\| = J \gg 1$ while all the other terms h_X have $\|h_X\| \leq 1$, the prescription above says that

we would have to divide the time step in $[J]$ pieces, and simulate each time slice. However, more careful inspection in the algorithm analysis tells us that one does not have to subdivide the time step for the entire system. For clarity in presentation, let us focus on a one-dimensional chain where the strong term h_{X_0} is at the middle of the chain. We then introduce a cut as in [Figure 1 \(a\)](#) at h_{X_0} . The purpose is to put the strong term into H_{bd} so that the truncation error in [Eq. \(5\)](#) is manifestly at most linear in J . Since the truncation error is exponential in ℓ , the factor of J in the error can be suppressed by increasing ℓ by $\mathcal{O}(\log J)$. After we confine the strong term in a block of size $2\ell_0 = \mathcal{O}(\log(JLT/\epsilon))$ in the middle of the chain, the rest of the blocks can be chosen to have size $\mathcal{O}(\log(LT/\epsilon))$ and do not have any strong term, and hence the time step can be as large as it would have been without the strong term. For the block with the strong term, we should subdivide the time step by a factor of $\mathcal{O}(J)$.

IV. REDUCING NUMBER OF LAYERS IN HIGHER DIMENSIONS

Although we have treated the spatial dimension D as a constant, the number of layers for unit time evolution is 3^D , which grows rather quickly in D , if we used the hyperplane decomposition as above. We can reduce this number by considering a different tessellation of the lattice.

To be concrete, let us explain the idea in two dimensions. Imagine a tiling of the two-dimensional plane using hexagons of diameter, say, 10ℓ . It is important that this hexagonal tiling is 3-colorable; one can assign one of three colors, red, green, and blue, to each of hexagons such that no two neighboring hexagons have the same color.

Let R, G, B be the unions of red, green, and blue hexagons, respectively. Each of R, G, B consists of well separated hexagons. Suppose we had implemented the time evolution $U(R \cup G)$ for $H_{R \cup G}$. Consider ℓ -neighborhood B^+ of B . $B^+ \cap (R \cup G)$ consists of separated rings of radius $\sim 6\ell$ and thickness $\sim \ell$. We can now apply [Lemma 4](#) to $R \cup G$ and B^+ , to complete the unit time evolution for the entire system $R \cup G \cup B$. The unitaries needed in addition to $U(R \cup G)$ are the backward time-evolution operator on $(R \cup G) \cap B^+$, which is a collection of disjoint unitaries on the rings, and the forward time-evolution operator on B^+ , which is a collection of disjoint unitaries on enlarged hexagons.

The time evolution $U(R \cup G)$ is constructed in a similar way. We consider an ℓ -neighborhood of G within $R \cup G$. The enlarged part $G^+ \cap R$ consists of line segments of thickness ℓ , and it is clear that $R \setminus G^+$ is ℓ -away from G . We can again apply [Lemma 4](#).

In summary, the algorithm under the 3-colored tessellation is (i) forward-evolve the blocks in

R , (ii) backward-evolve the blocks in $R \cap G^+$, (iii) forward-evolve the blocks in $G^+ \cap (R \cup G)$, (iv) backward-evolve the blocks in $(R \cup G) \cap B^+$, and (v) forward-evolve the blocks in B^+ .

In general, if the layout of qubits allows α -colorable tessellation, where $\alpha = 2, 3, 4, \dots$, such that the cells of the same color are well separated, then we can decompose unit time evolution into $2\alpha - 1$ layers by considering fattened cells of the tessellation. Here, being well-separated means that for any color c , the ℓ -neighborhood of a cell of color c does not intersect with any other cell of color c . The proof is by induction. When $\alpha = 2$, it is clear. For larger α , we implement the forward-evolution on the union A of $\alpha - 1$ colors using $2\alpha - 3$ layers by the induction hypothesis, and finish the evolution by backward-evolution on $A \cap B^+$, where B is the union of the last color and B^+ is the ℓ -neighborhood of B , and then forward-evolution on B^+ . This results in $2\alpha - 1$ layers in total.

A regular D -dimensional lattice can be covered with $D + 1$ colorable tessellation. One such coloring scheme is obtained by any triangulation of \mathbb{R}^D , and coloring each 0-cell by color “0”, and each 1-cell by color “1”, and so on, and finally fattening them.

For three dimensions, there exists a more “uniform” 4-colorable tessellation. Consider the body-centered cubic (BCC) lattice, spanned by basis vectors $(2, 0, 0)$, $(0, 2, 0)$, and $(1, 1, 1)$. Color each BCC lattice point $p = (x, y, z)$ by the rule $c = x + y + z \bmod 4$. The Voronoi tessellation associated with this colored BCC lattice is a valid 4-colored tessellation for our purpose. The shortest vector in the sublattice of the same color has length $2\sqrt{2} \simeq 2.828$, but a cell is contained in a ball of radius $\sqrt{5}/2 \simeq 1.118$, and therefore the cells of the same color are separated.

V. HEISENBERG MODEL BENCHMARK

We may gain some intuition in applying Lieb-Robinson bounds to quantum simulation with a concrete example. The Heisenberg model offers one useful benchmark [2] for the performance of various quantum simulation algorithms. In the case of 1D nearest-neighbor interactions with open boundary conditions, and where each spin is subject to an inhomogeneous magnetic field, its Hamiltonian is

$$H = \sum_{j=0}^{n-1} \underbrace{(X_j X_{j+1} + Y_j Y_{j+1} + Z_j Z_{j+1} + z_j Z_j)}_{h_j}, \quad (6)$$

where $\{X, Y, Z\}$ are the single-qubit Pauli operators. Though this Hamiltonian may be diagonalized in a closed form without the field term ($z_j = 0$), in the presence of non-uniform z_j this model can only be treated numerically in general.

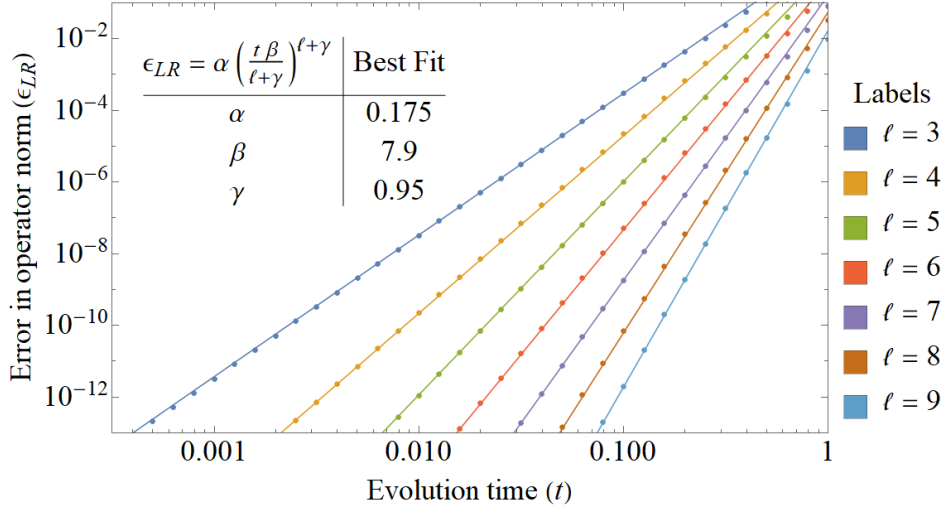


FIG. 2. Numerical test of $m = 1$ decomposition of the real-time evolution operator based on Lieb-Robinson bounds. The Hamiltonian is the antiferromagnetic one-dimensional Heisenberg model up to 11 spins in Eq. (6) with open boundary condition. The error of the decomposition in Eq. (7) is almost independent of the position a of the overlap within the system and is exponentially small in the overlap size ℓ . All lines plotted are the best-fit to $\epsilon_{LR} = \alpha \left(\frac{t\beta}{\ell+\gamma} \right)^{\ell+\gamma}$.

To recap, there are two sources of error in the entire quantum simulation algorithm for implementing time-evolution e^{-iTH} . One is from the decomposition of the full time-evolution operator e^{-iTH} using Lieb-Robinson bounds into $m = \mathcal{O}(Tn/\ell)$ blocks, and is bounded from above by $m\epsilon_{LR} = \mathcal{O}(me^{-\mu\ell})$ for some $\mu > 0$. The other is from approximate simulations of the block unitary using known algorithms such as [3, 5]. If each block is simulated up to error ϵ_{\square} , then the total error ϵ of the algorithm is at most $m(\epsilon_{LR} + \epsilon_{\square})$. Thus, we need $\ell = \mathcal{O}(\log(Tn/\epsilon))$.

Before proceeding, we require estimates of the Lieb-Robinson contribution to error ϵ_{LR} . By rescaling H and $1/T$ by the same constant factor to ensure that $\|h_j\| \leq 1$, this may be rigorously upper-bounded through Lemma 3. However, it is also reasonable to numerically obtain better constant factors in the scaling of ϵ_{LR} . Though simulation of the entire system of size n is classically intractable, ϵ_{LR} can be obtained by classically simulating small blocks of size $\mathcal{O}(\log(n))$, which is within the realm of feasibility. The decomposition ($m = 1$) is

$$\exp(-itH) \simeq \exp \left(-it \sum_{j < b} h_j \right) \exp \left(+it \sum_{j=a}^{b-1} h_j \right) \exp \left(-it \sum_{j \geq a} h_j \right) \quad (7)$$

so there are $\ell = b - a + 1$ spins in the overlap. We computed the error for a wide range of t up to $\ell = 9$, and observed that the error is almost independent of the position of the overlap, and is also exponentially small in ℓ . Note that the best fit $\epsilon_{LR} = \alpha \left(\frac{t\beta}{\ell+\gamma} \right)^{\ell+\gamma}$ in Figure 2 may be solved for

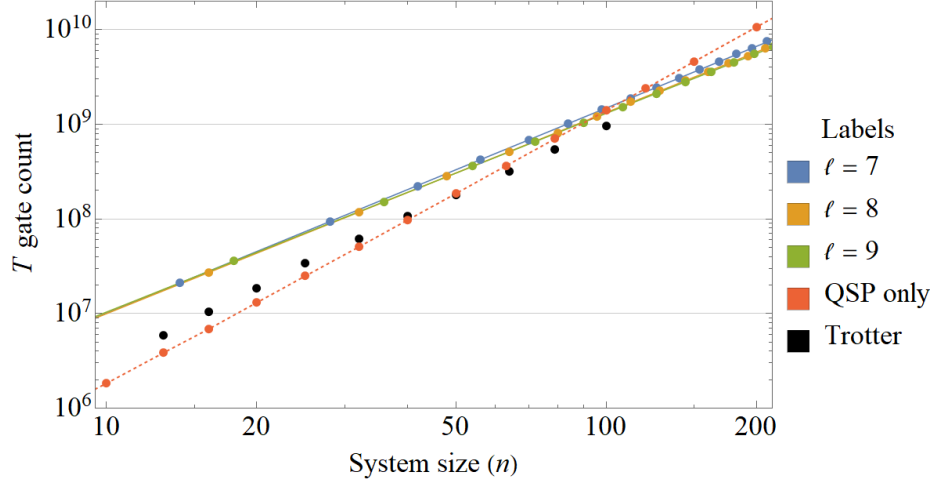


FIG. 3. T gate counts of simulating the Heisenberg model of Eq. (6) for time $T = n$, error $\epsilon = 10^{-3}$, and $h_j \in [-1, 1]$ chosen uniformly at random, using the Lieb-Robinson decomposition for overlap sizes of $\ell = 7, 8, 9$. Plotted for reference is the complexity $\tilde{\mathcal{O}}(n^3)$ of simulating the entire n -site system using Quantum Signal Processing (QSP) [4] without decomposing into blocks. Also plotted with data from [2] are the best-case gate counts using Lie-Trotter-Suzuki product formulas.

$\ell = \mathcal{O}(t + \log(1/\epsilon_{LR}))$, and is consistent with Lemma 4.

Using the recursive decomposition into blocks shown in Figure 1, we now simulate $m/2$ blocks of size ℓ and $m/2$ blocks of size 2ℓ , both for time t , and each with error $\epsilon_{\square} = \frac{\epsilon}{3m}$. Holding ℓ constant, we may use fit approximation of ϵ_{LR} to simultaneously solve for the number of blocks $m = \frac{2Tn}{\ell t}$ and the evolution time of each block t such that the Lieb-Robinson error contribution $\epsilon_{LR} = \frac{\epsilon}{3m}$. Note that we may also invert the ordering of sequential stacks in Eq. (7) to merge blocks of size 2ℓ . For instance,

$$\begin{aligned} e^{-itH} e^{-itH} &\simeq e^{(-it \sum_{j < b} h_j)} e^{(+it \sum_{j=a}^{b-1} h_j)} e^{(-it \sum_{j \geq a} h_j)} e^{(-it \sum_{j \geq a} h_j)} e^{(+it \sum_{j=a}^{b-1} h_j)} e^{(-it \sum_{j < b} h_j)} \\ &= e^{(-it \sum_{j < b} h_j)} e^{(+it \sum_{j=a}^{b-1} h_j)} e^{(-i2t \sum_{j \geq a} h_j)} e^{(+it \sum_{j=a}^{b-1} h_j)} e^{(-it \sum_{j < b} h_j)}. \end{aligned} \quad (8)$$

Excluding boundary cases, this leads to fewer blocks $m = \frac{3Tn}{2t\ell}$. Specifically, we may alternatively simulate $2m/3$ blocks of size ℓ for time t and $m/3$ blocks of size 2ℓ for time $2t$, and each with error $\epsilon_{\square} = \frac{\epsilon}{3m}$. Depending on the simulation algorithm used for each block, this may be slightly more efficient.

Similar to the benchmark in [2], we obtain explicit gate counts in the Clifford+ T basis in Figure 3 for simulating $e^{-iT\hat{H}}$ with $T = n$, error $\epsilon = 10^{-3}$, and $h_j \in [-1, 1]$ chosen uniformly at random. We implement each block with the combined quantum signal processing [4] and qubitization [5] simulation algorithm. An outline of this algorithm together with certain minor circuit optimizations

is discussed in [Appendix C](#).

VI. OPTIMALITY

In this section we prove a lower bound on the gate complexity of problem of simulating the time evolution of a time-dependent local Hamiltonian. (Recall that throughout this paper we use *local* to mean geometrically local.) This lower bound matches, up to logarithmic factors, the gate complexity of the algorithm presented above. Note that unlike previous lower bounds on Hamiltonian simulation [\[15, 16, 18\]](#), which prove lower bounds on query complexity, this is a lower bound on the number of gates required to approximately implement the time-evolution unitary. For concreteness, we focus on a 1-dimensional time-dependent local Hamiltonian in this section, although the lower bound extends to other constant dimensions with minor modifications.

Before stating the result formally, let us precisely define the class of Hamiltonians for which we prove the lower bound. We say a Hamiltonian $H(t)$ acting on n qubits is a “piecewise constant 1D Hamiltonian” if $H(t) = \sum_{j=1}^{n-1} H_j(t)$, where $H_j(t)$ is only supported on qubits j and $j+1$ with $\max_t \|H_j(t)\| = \mathcal{O}(1)$, and there is a time slicing $0 = t_0 < t_1 < \dots < t_M = T$ where $t_m - t_{m-1} \leq 1$ and $M = \mathcal{O}(T)$ such that $H(t)$ is time-independent within each time slice.

For such Hamiltonians, the time evolution operator for time T can be simulated with error at most ϵ using [Theorem 1](#) with $\mathcal{O}(Tn \operatorname{polylog}(Tn/\epsilon))$ 2-qubit local gates (i.e., the 2-qubit gates only act on adjacent qubits). In particular, for any constant error, the simulation only requires $\tilde{\mathcal{O}}(Tn)$ 2-qubit local gates.² We prove a matching lower bound, where the lower bound even holds against circuits that may use non-local (i.e., acting on non-adjacent qubits) 2-qubit gates from a possibly infinite gate set and unlimited ancilla qubits.

Theorem 5. *For any integers n and T such that $T \leq 4^n$, there exists a piecewise constant bounded 1D Hamiltonian $H(t)$ on n qubits, such that any quantum circuit that approximates the time evolution due to $H(t)$ for time T to constant error must use $\tilde{\Omega}(Tn)$ 2-qubit gates. The quantum circuit may use unlimited ancilla qubits and the gates may be non-local and come from a possibly infinite gate set.*

Note that this lower bound only holds for $T \leq 4^n$, because any unitary on n qubits can be implemented with $\tilde{\mathcal{O}}(4^n)$ 2-qubit local gates [\[19, 20\]](#).

² As usual, $\tilde{\mathcal{O}}(f)$ and $\tilde{\Omega}(f)$ mean $\mathcal{O}(f \operatorname{polylog} f)$ and $\Omega(f / \operatorname{polylog} f)$, respectively, for any function f .

We can also strengthen our lower bound to work in the situation where we are only interested in measuring a local observable at the end of the simulation. The simulation algorithm presented in [Theorem 1](#) provides a strong guarantee: the output state is ϵ -close to the ideal output state in trace distance. Trace distance captures distinguishability with respect to arbitrary measurements, but for some applications it might be sufficient for the output state to be close to the ideal state with respect to local measurements only. We show that even in this limited measurement setting, it is not possible to speed up our algorithm in general. In fact, our lower bound works even if the only local measurement performed is a computational basis measurement on the first output qubit.

Theorem 6. *For any integers n and T such that $1 \leq n \leq T \leq 2^n$, there exists a piecewise constant bounded 1D Hamiltonian $H(t)$ on n qubits, such that any quantum circuit that approximates the time evolution due to $H(t)$ for time T to constant error on any local observable must use $\tilde{\Omega}(Tn)$ 2-qubit gates. If $T \leq n$, we have a lower bound of $\tilde{\Omega}(T^2)$ gates. (The quantum circuit may use unlimited ancilla qubits and the gates may be non-local and come from a possibly infinite gate set.)*

Note that the fact that we get a weaker lower bound of $\tilde{\Omega}(T^2)$ when $T \leq n$ is not a limitation, but reflects the fact that small time evolutions are actually easier to simulate when the measurement is local. To see this, consider first simulating the time evolution using the algorithm in [Theorem 1](#). This yields a circuit with $\tilde{\mathcal{O}}(Tn)$ 2-qubit local gates. But if we only want the output of a local measurement after time T , qubits that are far away from the measured qubits cannot affect the output, since the circuit only consists of 2-qubit local gates. Hence we can simply remove all gates that are more than distance equal to the depth of the circuit, $\tilde{\mathcal{O}}(T)$, away from the measured qubits. We are then left with a circuit that uses $\tilde{\mathcal{O}}(T^2)$ gates, matching the lower bound in [Theorem 6](#).

A. Lower bound proofs

We now prove [Theorem 5](#) and [Theorem 6](#), starting with [Theorem 6](#). This lower bound follows from the following three steps. First, in [Lemma 7](#), we observe that for every depth- T quantum circuit on n qubits that uses local 2-qubit gates, there exists a Hamiltonian $H(t)$ of the above form such that time evolution due to $H(t)$ for time T is equal to applying the quantum circuit. Then, in [Lemma 8](#) we show that the number of distinct Boolean functions on n bits computed by such quantum circuits is at least exponential in $\tilde{\Omega}(Tn)$, where we say a quantum circuit has computed a Boolean function if its first output qubit is equal to the value of the Boolean function with high probability. Finally, in [Lemma 9](#) we observe that the maximum number of Boolean functions that

can be computed (to constant error) by the class of quantum circuits with G arbitrary non-local 2-qubit gates from any (possibly infinite) gate set is exponential in $\tilde{\mathcal{O}}(G \log n)$. Since we want this class of circuits to be able to simulate all piecewise constant bounded 1D Hamiltonians for time T , we must have $G = \tilde{\Omega}(Tn)$.

Lemma 7. *Let U be a depth- T quantum circuit on n qubits that uses local 2-qubit gates from any gate set. Then there exists a piecewise constant bounded 1D Hamiltonian $H(t)$ such that the time evolution due to $H(t)$ for time T exactly equals U .*

Proof. We first prove the claim for a depth-1 quantum circuit. This yields a Hamiltonian $H(t)$ that is defined for $t \in [0, 1]$, whose time evolution for unit time equals the given depth-1 circuit. Then we can apply the same argument to each layer of the circuit, obtaining Hamiltonians valid for times $t \in [1, 2]$, and so on, until $t \in [T-1, T]$. This yields a Hamiltonian $H(t)$ defined for all time $t \in [0, T]$ whose time evolution for time T equals the given unitary. If the individual terms in a given time interval have bounded spectral norm, then so will the Hamiltonian defined for the full time duration.

For a depth 1 circuit with local 2-qubit gates, since the gates act on disjoint qubits we only need to solve the problem for one 2-qubit unitary and sum the resulting Hamiltonians. Consider a unitary U_j that acts on qubits j and $j+1$. By choosing $H_j = i \log U_j$, we can ensure that $e^{-iH_j} = U_j$ and $\|H_j\| = \mathcal{O}(1)$.

The overall Hamiltonian is now piecewise constant with T time slices. \square

Note that it is also possible to use a similar construction to obtain a Hamiltonian that is continuous (instead of being piecewise constant) with a constant upper bound on the norm of the first derivative of the Hamiltonian.

Lemma 8. *For any integers n and T such that $1 \leq n \leq T \leq 2^n$, the number of distinct Boolean functions $f : \{0, 1\}^n \rightarrow \{0, 1\}$ that can be computed by depth- T quantum circuits on n qubits that use local 2-qubit gates from a finite gate set is at least $2^{\tilde{\Omega}(Tn)}$.*

Proof. We first divide the n qubits into groups of $k = \log_2 T$ qubits, which is possible since $T \leq 2^n$. On these k qubits, we will show that it is possible to compute $2^{\tilde{\Omega}(T)}$ distinct Boolean functions with a depth T circuit that uses local 2-qubit gates. One way to do this is to consider all Boolean functions on $k' < k$ bits. Any Boolean function f_x that evaluates to $f_x(x) = 1$ on exactly one input x of size k' can be computed with a circuit of $\tilde{\mathcal{O}}(k')$ gates and $\tilde{\mathcal{O}}(k')$ depth using only 2-qubit gates and 1 ancilla qubit in addition to one output qubit [19, Corollary 7.4]. An arbitrary Boolean function

$f : \{0, 1\}^{k'} \rightarrow \{0, 1\}$ is a sum of such functions: $f = \sum_{x \in f^{-1}(1)} f_x = \bigoplus_{x \in f^{-1}(1)} f_x$. Implementing all f_x for $x \in f^{-1}(1)$ in serial using a common output qubit, we obtain a circuit for the full function f . Since $f^{-1}(1)$ consists at most $2^{k'}$ bit strings, this will yield a circuit of size $\tilde{\mathcal{O}}(2^{k'})$ and depth $\tilde{\mathcal{O}}(2^{k'})$. Making all the gates local using SWAP gates does not change these expressions by more than a log factor in the exponent. By choosing $k' = k - \Theta(\log k)$, we can compute all Boolean functions on k' bits with depth at most T . Since there are $2^{2^{k'}} = 2^{\tilde{\Omega}(T)}$ distinct Boolean functions on k' bits, we have shown that circuits with depth T using $k = \log_2 T$ qubits can compute at least $2^{\tilde{\Omega}(T)}$ distinct Boolean functions.

We can compute $2^{\tilde{\Omega}(T)}$ distinct Boolean functions on each of the n/k blocks of k qubits to obtain $(2^{\tilde{\Omega}(T)})^{n/k} = 2^{\tilde{\Omega}(Tn)}$ distinct Boolean functions with n/k outputs. I.e., we have computed a function $\{0, 1\}^n \rightarrow \{0, 1\}^{n/k}$. Since we want to obtain a single-output Boolean function, as the overall goal is to prove lower bounds against simulation algorithms correct on local measurements, we combine these Boolean functions into one. We do this by computing the parity of all the outputs of these n/k Boolean functions using CNOT gates. Computing the parity uses at most n 2-qubit local gates and has depth n . The circuit now has depth $T + n \leq 2T$ and by rescaling T we can make this circuit have depth T , while retaining the lower bound of $2^{\tilde{\Omega}(Tn)}$ distinct Boolean functions.

Unfortunately, after taking the parity of these n/k functions, it is not true that the resulting functions are all distinct. For example, the parity of functions $f(x)$ and $g(y)$ is a new function $f(x) \oplus g(y)$, which also happens to be the parity of the functions $\neg f(x)$ and $\neg g(y)$. To avoid this overcounting of functions, we do not use all possible functions on k' bits in the argument above, but only all those functions that map the all-zeros input to 0. This only halves the total number of functions, which does not change the asymptotic expressions above. With this additional constraint, it is easy to see that if $f(x) \oplus g(y) = f'(x) \oplus g'(y)$, this implies that f and f' are the same, by fixing y to be the all-zeros input, and similarly that g and g' are the same. \square

Lemma 9. *The number of Boolean functions $f : \{0, 1\}^n \rightarrow \{0, 1\}$ that can be computed with high probability by quantum circuits with unlimited ancilla qubits using G non-local 2-qubit gates from any gate set is at most $2^{\tilde{\mathcal{O}}(G \log n)}$.*

Proof. We say a quantum circuit U computes a Boolean function $f : \{0, 1\}^n \rightarrow \{0, 1\}$ with high probability if measuring the first output qubit of $U|x_1 x_2 \cdots x_n 0 \cdots 0\rangle$ yields $f(x)$ with probability at least $2/3$. First we note that if a circuit U with G arbitrary 2-qubit gates from any gate set computes a Boolean function with probability at least $2/3$, then there is another circuit with $\tilde{\mathcal{O}}(G)$ gates from a finite 2-qubit non-local gate set that computes the same function with probability

at least $2/3$. We do this by first boosting the success probability of the original circuit using an ancilla qubit to a constant larger than $2/3$ and then invoking the Solovay–Kitaev theorem [21] to approximate each gate in this circuit to error $\mathcal{O}(1/G)$ with a circuit from a finite gate set of 2-qubit gates. This increases the circuit size to $\tilde{\mathcal{O}}(G)$ gates. Since each gate has error $\mathcal{O}(1/G)$, the overall error is only a constant, and the new circuit approximates computes the Boolean function f with high probability.

We now have to show that the number of Boolean functions on n bits computed by a circuit with $\tilde{\mathcal{O}}(G)$ non-local 2-qubit gates from a finite gate set is at most $2^{\tilde{\mathcal{O}}(G \log n)}$. To do so, we simply show that the total number of distinct circuits with $\tilde{\mathcal{O}}(G)$ non-local 2-qubit gates from a finite gate set is at most $2^{\tilde{\mathcal{O}}(G \log n)}$.

First observe that a circuit with $\tilde{\mathcal{O}}(G)$ gates can only use $\tilde{\mathcal{O}}(G)$ ancilla qubits, since each 2-qubit gate can interact with at most 2 new ancilla qubits. Furthermore, the depth of a circuit cannot be larger than the number of gates in the circuit. Let us now upper bound the total number of quantum circuits of this form. Each such circuit can be specified by listing the location of each gate and which gate it is from the finite gate set. Specifying the latter only needs a constant number of bits since the gate set is finite, and the location can be specified using the gate’s depth, and the labels of the two qubits it acts on. The depth only requires $\mathcal{O}(\log G)$ bits to specify, and since there are at most $n + \tilde{\mathcal{O}}(G)$ qubits, this only needs $\mathcal{O}(\log n + \log G)$ bits to specify. In total, since there are $\tilde{\mathcal{O}}(G)$ gates, the entire circuit can be specified with $\tilde{\mathcal{O}}(G \log n)$ bits. Finally, since any such circuit can be specified with $\tilde{\mathcal{O}}(G \log n)$ bits, there can only be $2^{\tilde{\mathcal{O}}(G \log n)}$ such circuits. \square

Proof of Theorem 6. Suppose that any piecewise constant bounded 1D Hamiltonian on n qubits can be simulated for time T using G 2-qubit non-local gates from any (possibly infinite) gate set. Then using Lemma 7 and Lemma 8, we can compute at least $2^{\tilde{\Omega}(Tn)}$ distinct Boolean functions using such Hamiltonians. By assumption, each of these Boolean functions can be approximately computed by a circuit with G gates. Now invoking Lemma 9, we know that such circuits can compute at most $2^{\tilde{\mathcal{O}}(G \log n)}$ n -bit Boolean functions. Hence we must have $G \log n = \tilde{\Omega}(Tn)$, which yields $G = \tilde{\Omega}(Tn)$.

The proof for $T \leq n$ follows in a black-box manner from the first part of the theorem statement by only using T out of the n available qubits. In this case the first part of the theorem applies and yields a lower bound of $\tilde{\Omega}(T^2)$. \square

We now prove Theorem 5, which follows a similar outline. The first step is identical, and we can reuse Lemma 7. For the next step, instead of counting distinct Boolean functions, we count the

total number of “distinct” unitaries. Unlike Boolean functions on n bits, there are infinitely many unitaries on n qubits. Hence we count unitaries that are “distinguishable.” Formally, we say U and V are distinguishable if they are some constant, say 0.1 for concreteness, apart in diamond norm. This is equivalent to the existence of a state $|\psi\rangle$ such that $U|\psi\rangle$ and $V|\psi\rangle$ have trace distance 0.1. In [Lemma 10](#) we show that the number of distinguishable unitaries computed by quantum circuits on n qubits with depth T is exponential in $\tilde{\Omega}(Tn)$. As before, we then show that the maximum number of distinguishable unitaries that can be computed (to constant error) by the class of quantum circuits with G arbitrary non-local 2-qubit gates from any (possibly infinite) gate set is exponential in $\tilde{\mathcal{O}}(G \log n)$.

Lemma 10. *For any integer n and integer $n \leq T \leq 4^n$, there exists a set of unitaries of size $2^{\tilde{\Omega}(Tn)}$, such that every unitary in the set can be computed by a depth- T quantum circuit on n qubits that uses local 2-qubit gates from a finite gate set, and the diamond norm distance between any $U \neq V$ from this set is at least 0.1.*

Proof. We divide the n qubits into groups of $k = \log_4 T$ qubits, which is possible since $T \leq 4^n$. On these k qubits, we will compute $2^{\tilde{\Omega}(T)}$ distinguishable unitaries (i.e., unitaries that are at least distance 0.1 apart from each other) with a depth T circuit that uses local 2-qubit gates. We can do this by considering a maximal set of unitaries on k' qubits that is distinguishable. More precisely, on k' qubits there exist $2^{\Omega(4^{k'})}$ unitaries such that each pair of unitaries is at least distance 0.1 apart; see e.g. [\[22\]](#). (This follows from the fact that in the group of $d \times d$ unitaries with metric induced by operator norm, a ball of radius 0.1 has volume exponentially small in d^2 .) We know that any unitary on k' qubits can be exactly written as a product of $\tilde{\mathcal{O}}(4^{k'})$ arbitrary 2-qubit gates [\[19, 20\]](#). Making these gates local and from a finite gate set only adds polynomial factors in k' . By choosing $k' = k - \Theta(\log k)$, we can compute this set of $2^{\Omega(4^{k'})} = 2^{\tilde{\Omega}(T)}$ distinguishable unitaries with depth at most T .

Since we can compute $2^{\tilde{\Omega}(T)}$ pairwise-distant unitaries on each of the n/k blocks of k qubits, we can compute $(2^{\tilde{\Omega}(T)})^{n/k} = 2^{\tilde{\Omega}(Tn)}$ unitaries on all n qubits by considering all possible combinations of unitaries on the different blocks. Finally, if U and V are distinguishable, then so are $U \otimes X$ and $V \otimes Y$, since the distinguisher can simply ignore the second register. \square

Lemma 11. *Let S be a set of distinguishable unitaries (i.e., the diamond norm distance between any $U \neq V$ from this set is at least 0.1). Then if any unitary in S can be computed by a quantum circuit with G non-local 2-qubit gates from any gate set, then $|S| = 2^{\tilde{\mathcal{O}}(G \log n)}$.*

Proof. This proof is essentially the same as that of [Lemma 9](#). We first observe that if a circuit over an arbitrary gate set computes a unitary U , we can approximate it to error less than 0.04 using the Solovay–Kitaev theorem and increase the circuit size to $\tilde{\mathcal{O}}(G)$ gates. Importantly, since the unitaries are a distance 0.1 apart, one circuit cannot simultaneously approximate two different unitaries to error 0.04. Then exactly the same counting argument as in [Lemma 9](#) shows there can only be $2^{\tilde{\mathcal{O}}(G \log n)}$ such circuits. \square

Proof of Theorem 5. Suppose that any piecewise constant bounded local Hamiltonian on n -qubits could be simulated for time T using G 2-qubit non-local gates from any (possibly infinite) gate set. Then using [Lemma 7](#) and [Lemma 10](#), we can produce a set S of distinguishable unitaries of size $2^{\tilde{\Omega}(Tn)}$. By assumption, each of these unitaries can be approximately computed by a circuit with G non-local 4-qubit gates. Now invoking [Lemma 9](#), we know that such circuits can approximate at most $2^{\tilde{\mathcal{O}}(G \log n)}$ distinguishable unitaries on n qubits. Hence we must have $G \log n = \tilde{\Omega}(Tn)$, which yields $G = \tilde{\Omega}(Tn)$. \square

VII. DISCUSSION

We have only analyzed local Hamiltonians on (hyper)cubic lattices embedded in some Euclidean space, but Lieb-Robinson bounds with exponential dependence on the separation distance hold more generally. However, on more general graphs, it may be more difficult to find an appropriate decomposition that gives a small error; this must be analyzed for each graph. One advantage of the method here is that the accuracy improves for smaller Lieb-Robinson velocity. This can occur if the terms in the Hamiltonian have a small commutator; see [Appendix A](#).

Application to fermions is straightforward since Hamiltonian terms always have fermion parity even. If one represents a fermionic Hamiltonian by the Jordan-Wigner transformation (the representation of Clifford algebra), any local operator of odd fermion parity has large support over the qubits, but every local term of the Hamiltonian has local support over the qubits.

If we use quantum signal processing based algorithms [\[4, 5\]](#) to implement the blocks of size $\mathcal{O}(\ell^D)$, then we need $\mathcal{O}(\log \ell)$ ancilla qubits for a block. Thus, if we do not mind implementing them all in serial, then it follows that the number of ancillas needed is $\mathcal{O}(\log \log(TL/\epsilon))$, which is much smaller than what would be needed if the quantum signal processing algorithm was directly used to simulate the full system.

The decomposition based on Lieb-Robinson bounds looks very similar to higher order Lie-Trotter-Suzuki formulas. The difference is in the fact that the overlap is chosen to be larger and

larger (though very slowly) as the simulated spacetime volume increases. This might guide us to understand why Lie-Trotter-Suzuki formulas work well empirically.

Appendix A: Lieb-Robinson Bounds with Bounded Commutators

1. Introduction and Assumptions

One advantage of the method described in this paper is that if the Lieb-Robinson velocity is small, then the method becomes more accurate. One case in which this occurs is if the terms in the Hamiltonian have a small commutator with each other. This section considers the Lieb-Robinson velocity under such a small commutator assumption. Note that Trotter-Suzuki methods also improve in accuracy if the Hamiltonian terms have a small commutator, but many other time-simulation methods do not.

Consider a Hamiltonian $H = \sum_X h_X$, where each X represents some set of sites and the sum is over all possible subsets of the lattice. h_X is a Hermitian operator obeying a commutator condition

$$\|[h_X, h_Y]\| \leq \eta \|h_X\| \|h_Y\| \quad (\text{A1})$$

for all X, Y for some $0 \leq \eta \leq 2$.

We will additionally impose some locality assumption on H . A convenient one is exponential decay in the following form. Introduce a metric $\text{dist}(x, y)$ between pairs of sites x, y . Assume that there are constants $\zeta, \mu > 0$ such that for any site x ,

$$\sum_{X \ni x} \|h_X\| |X|^2 \exp(\mu \text{diam}(X)) \leq \zeta < \infty \quad (\text{A2})$$

where $|X|$ denotes the cardinality of set X . The assumption (A2) will not be used until subsection A 3; we will indicate where it is used as many of the early bounds do not use this assumption and only use Eq. (A1). This assumption is slightly stronger than previous exponential decay assumptions such as in Ref. [11] as we have $|X|^2$ rather than $|X|$. The reason for this will be clear later. Note that we do not impose $\|h_X\| \leq 1$ in this appendix; the strength of interaction is bounded only through (A2).

The main result that we will prove under these assumptions is:

Lemma 12. *Assume that assumptions (A1, A2) hold. For any operator O , let $O(t) = O(t; H) = \exp(iHt)O\exp(-iHt)$. Then, for any operator A supported on a set X and operator B supported*

on a set Y we have

$$\|[A(t), B]\| \leq \frac{2}{\sqrt{\eta}} \|A\| \cdot \|B\| \left(\exp\left(\zeta|t|\sqrt{8\eta}\right) - 1 \right) \sum_{x \in X} \exp(-\mu \operatorname{dist}(x, Y)). \quad (\text{A3})$$

Let v_{LR} be chosen greater than $\zeta\sqrt{8\eta}/\mu$. Then, for large t , at fixed $\operatorname{dist}(X, Y)/t \leq v_{LR}$, for bounded $|X|$, the above bound tends to zero, giving a Lieb-Robinson velocity proportional to $\sqrt{\eta}$.

A Lieb-Robinson velocity proportional to $\sqrt{\eta}$ might initially be surprising: one might hope to have a bound proportional to η . However, one can see that this is the best possible under these assumptions. Consider any local Hamiltonian $H = \sum_X h_X^0$ (without a commutator condition) with $\|h_X^0\|$ of order unity and Lieb-Robinson velocity v_{LR}^0 also of order unity. Now, consider a new Hamiltonian $H = \sum_X h_X$ with $h_X = 1 + \sqrt{\eta}h_X^0$; here 1 simply denotes the identity operator. Then, the commutator of any two terms is proportional to η , while the norm of the terms is still of order 1 and the Lieb-Robinson velocity is proportional to $\sqrt{\eta}$. If the reader does not like adding the identity to define h_X as a way of ensuring $\|h_X\| \sim 1$, one could instead add some other exactly commuting terms of norm 1 which act on some additional degrees of freedom.

In the proof below, we use notations as if the Hamiltonian was time-independent. However, [Lemma 12](#) is valid if Hamiltonian is a piecewise continuous function of time, provided that assumptions [\(A1,A2\)](#) hold for all time.

2. Bound on Commutator Assuming Eq. [\(A1\)](#)

We wish to bound

$$\|[\exp(iHt)A_X \exp(-iHt), B_Y]\|. \quad (\text{A4})$$

where A_X is supported on X and B_Y is supported on Y . Define

$$C_B(X, t) = \sup_{A \in \mathcal{A}_X: \|A\| \leq 1} \|[A(t), B]\|, \quad (\text{A5})$$

$$D_B(X, t) = \|[h_X(t), B]\| \quad (\text{A6})$$

where \mathcal{A}_X is the algebra of operators supported on X . For any two sets X and Y of sites we will write $X \sim Y$ in place of $X \cap Y \neq \emptyset$. Also, the notation $Z_1 \sim Z_2 \sim \dots \sim Z_m$ will mean that $Z_j \sim Z_{j+1}$ for every $j = 1, \dots, m-1$. This does *not* necessarily mean that $Z_j \sim Z_k$ for $j+1 < k$. For any set X , define I_X as

$$I_X = \sum_{Z: Z \sim X} h_Z. \quad (\text{A7})$$

Let dt be a small positive real number. We consider a finite system so that H has finite operator norm; the bounds that we prove will be uniform in system size after we take dt to zero. We have

$$\begin{aligned}
& \| [A(t + dt), B] \| \tag{A8} \\
&= \| [A(dt), B(-t)] \| \\
&= \| [\exp(iI_X dt) A \exp(-iI_X dt), B(-t)] \| + \mathcal{O}(dt^2) \\
&= \| [A, \exp(-iI_X dt) B(-t) \exp(iI_X dt)] \| + \mathcal{O}(dt^2) \\
&= \| [A, B(-t) - idt[I_X, B(-t)]] \| + \mathcal{O}(dt^2) \\
&\leq \| [A, B(-t)] \| + 2dt \| A \| \cdot \| [I_X, B(-t)] \| + \mathcal{O}(dt^2) \\
&\leq \| [A, B(-t)] \| + 2dt \| A \| \sum_{Z:Z \sim X} \| [h_Z, B(-t)] \| + \mathcal{O}(dt^2)
\end{aligned}$$

By definitions of $C_B(X, t)$ and $D_B(X, t)$, it follows that

$$C_B(X, t + dt) \leq C_B(X, t) + 2dt \sum_{Z:Z \sim X} D_B(Z, t) + \mathcal{O}(dt^2). \tag{A9}$$

Hence, for any positive integer n ,

$$C_B(X, t) \leq C_B(X, 0) + \frac{1}{n} \sum_{j=0}^n \sum_{Z:Z \sim X} 2D_B(Z, tj/n) + \mathcal{O}(1/n). \tag{A10}$$

For finite operator norm of H , the above expression converges to an integral as $n \rightarrow \infty$, so

$$C_B(X, t) \leq C_B(X, 0) + \sum_{Z:Z \sim X} 2 \int_0^{|t|} D_B(Z, s) ds. \tag{A11}$$

Also, we have

$$\begin{aligned}
& \| [h_X(t + dt), B] \| \tag{A12} \\
&= \| [h_X(dt), B(-t)] \| \\
&= \| [h_X, B(-t)] + idt [[I_X, h_X], B(-t)] \| + \mathcal{O}(dt^2) \\
&\leq \| [h_X, B(-t)] \| + dt \sum_{Z:Z \sim X} \| [[h_Z, h_X], B(-t)] \|.
\end{aligned}$$

By definitions of $C_B(X, t)$ and $D_B(X, t)$ and assumption (A1), it follows that

$$D_B(X, t + dt) \leq D_B(X, t) + 2dt \sum_{Z:Z \sim X} \eta \| h_Z \| \cdot \| h_X \| C_B(Z \cup X, t). \tag{A13}$$

Hence,

$$D_B(X, t) \leq D_B(X, 0) + \sum_{Z:Z \sim X} 2\eta \int_0^{|t|} \| h_Z \| \cdot \| h_X \| C_B(Z \cup X, s) ds. \tag{A14}$$

Note that for arbitrary set Z of sites

$$\begin{aligned} C_B(Z, 0) &\leq 2 \|B\| \delta_{Z \sim Y}, \\ D_B(Z, 0) &\leq 2 \|B\| \|h_Z\| \delta_{Z \sim Y} \end{aligned} \quad (\text{A15})$$

where $\delta_{\mathbb{P}} = 1$ if the predicate \mathbb{P} is true and $\delta_{\mathbb{P}} = 0$ otherwise. Since X and Y are arbitrary, we may use Eq. (A14) in Eq. (A11); for any sets Z_{j-2}, Z_{j-1} we have:

$$\begin{aligned} &\frac{C_B(Z_{j-2} \cup Z_{j-1}, s_{j-1})}{2 \|B\|} \\ &\leq \delta_{(Z_{j-2} \cup Z_{j-1}) \sim Y} \\ &+ (2s_{j-1}) \sum_{Z_j: (Z_{j-2} \cup Z_{j-1}) \sim Z_j \sim Y} \|h_{Z_j}\| \\ &+ \eta \cdot 2^2 \int_0^{s_{j-1}} ds_j \int_0^{s_j} ds_{j+1} \sum_{Z_j, Z_{j+1}: (Z_{j-2} \cup Z_{j-1}) \sim Z_j \sim Z_{j+1}} \|h_{Z_j}\| \|h_{Z_{j+1}}\| \frac{C_B(Z_j \cup Z_{j+1}, s_{j+1})}{2 \|B\|} \end{aligned} \quad (\text{A16})$$

where $s_{j-1} \geq 0$. This is our fundamental recursive inequality. Assuming $X \cap Y = \emptyset$ and setting $Z_{-1} = \emptyset, Z_0 = X$, we have

$$\begin{aligned} \frac{C_B(X, t)}{2 \|B\|} &\leq (2|t|) \sum_{Z_1: X \sim Z_1 \sim Y} \|h_{Z_1}\| \\ &+ \eta \frac{(2|t|)^2}{2!} \sum_{Z_1, Z_2: X \sim Z_1 \sim Z_2 \sim Y} \|h_{Z_1}\| \|h_{Z_2}\| \\ &+ \eta \frac{(2|t|)^3}{3!} \sum_{Z_1, Z_2: X \sim Z_1 \sim Z_2} \|h_{Z_1}\| \|h_{Z_2}\| \sum_{Z_3: (Z_1 \cup Z_2) \sim Z_3 \sim Y} \|h_{Z_3}\| \\ &+ \eta^2 \frac{(2|t|)^4}{4!} \sum_{Z_1, Z_2: X \sim Z_1 \sim Z_2} \|h_{Z_1}\| \|h_{Z_2}\| \sum_{Z_3, Z_4: (Z_1 \cup Z_2) \sim Z_3 \sim Z_4 \sim Y} \|h_{Z_3}\| \|h_{Z_4}\| \\ &+ \dots \end{aligned} \quad (\text{A17})$$

The above equation has the following pattern: On the k -th line, there is a prefactor of $(2|t|)^k \eta^{[k/2]} / k!$. Then, there is a sum over Z_1, Z_2, \dots, Z_k of $\prod_j \|h_{Z_j}\|$, subject to the constraints that for any $1 \leq j \leq k$

$$\begin{aligned} (Z_{j-2} \cup Z_{j-1}) &\sim Z_j \text{ if } j \text{ is odd,} \\ Z_{j-1} &\sim Z_j \text{ if } j \text{ is even, and} \\ Z_k &\sim Y. \end{aligned} \quad (\text{A18})$$

3. Lieb-Robinson Velocity

We now use assumption (A2), especially the following consequences.

Proposition 13. For arbitrary sets P, Q, R, S of sites

$$\sum_{Q:P \sim Q \sim S} \|h_Q\| \leq \zeta \sum_{p \in P} e^{-\mu \text{ dist}(p, S)}, \quad (\text{A19})$$

$$\sum_{Q:P \sim Q} \|h_Q\| |Q|^2 e^{-\mu \text{ dist}(Q, S)} \leq \zeta \sum_{p \in P} e^{-\mu \text{ dist}(p, S)}, \quad (\text{A20})$$

$$\sum_{Q,R:P \sim Q \sim R \sim S} \|h_Q\| \|h_R\| \leq \zeta^2 \sum_{p \in P} e^{-\mu \text{ dist}(p, S)}, \quad (\text{A21})$$

$$\sum_{Q,R:P \sim Q \sim R} |Q \cup R| \|h_Q\| \|h_R\| e^{-\mu \text{ dist}(Q \cup R, S)} \leq 2\zeta^2 \sum_{p \in P} e^{-\mu \text{ dist}(p, S)}. \quad (\text{A22})$$

Here, $\sum_{p \in P} e^{-\mu \text{ dist}(p, S)} \leq |P| e^{-\mu \text{ dist}(P, S)}$.

Proof. (A19): Observe $\sum_{Q:P \sim Q \sim S} \leq \sum_{p \in P} \sum_{Q:p \in Q \sim S}$ whenever the summand is nonnegative. Using assumption (A2) and $\text{diam}(Q) \geq \text{dist}(p, S)$ when $p \in Q \sim S$, we have an upper bound as $\sum_p \sum_{Q:p \in Q \sim S} \|h_Q\| e^{\mu \text{ diam}(Q) - \mu \text{ dist}(p, S)} \leq \zeta \sum_p e^{-\mu \text{ dist}(p, S)}$.

(A20): Similarly, we use that $\text{diam}(Q) + \text{dist}(Q, S) \geq \text{dist}(p, S)$ when $p \in Q$ by triangle inequality of the metric.

(A21): Use (A19) for the sum over R and then use (A20) for the sum over Q .

(A22): Use $|Q \cup R| \leq |Q| \cdot |R|$ since $Q \sim R$. We then separately bound two cases where (i) $\text{dist}(Q \cup R, S) = \text{dist}(R, S)$ and (ii) $\text{dist}(Q \cup R, S) = \text{dist}(Q, S)$. The sum of (i) and (ii) is an upper bound to the original sum. For case (i), we use (A20) for the sum over R to have an upper bound $\zeta \sum_{Q:P \sim Q} |Q|^2 \|h_Q\| e^{-\mu \text{ dist}(Q, S)}$, and then use (A20) again for the sum over Q to have an upper bound $\zeta^2 |P| e^{-\mu \text{ dist}(P, S)}$. For case (ii), we use either (A19) or (A20) to sum over R , which gives $\zeta \sum_{Q:P \sim Q} |Q|^2 \|h_Q\| e^{-\mu \text{ dist}(Q, S)}$, and then use (A20). \square

Now, we can use (A19) for the innermost sum in any odd- k -th line of (A17), and (A21) for that in any even- k -th line. Once the innermost sum is bounded, we use (A22) for $\lfloor (k-1)/2 \rfloor$ times. This is the point at which the dependence on $|X|^2$ in assumption (A2) is necessary. Therefore, the k -th line is bounded by

$$\frac{(2|t|)^k}{k!} \eta^{\lfloor k/2 \rfloor} 2^{\lfloor (k-1)/2 \rfloor} \zeta^k \sum_{x \in X} \exp(-\mu \text{ dist}(x, Y)). \quad (\text{A23})$$

Summing over k we find that

$$C_B(X, t) \leq \frac{2}{\sqrt{\eta}} \|B\| \left(\exp \left(\zeta |t| \sqrt{8\eta} \right) - 1 \right) \sum_{x \in X} \exp(-\mu \text{ dist}(x, Y)), \quad (\text{A24})$$

so that Lemma 12 follows.

4. Proof of Lemma 3

A slight modification of the previous section proves Lemma 3. Recall that $H_\Omega = \sum_{Z:Z \subseteq \Omega} h_Z$, and it suffices to assume $X \subset \Omega$. Then,

$$\begin{aligned} \|A_X(t; H_\Omega) - A_X(t; H)\| &= \left\| \int_0^t ds \partial_s (U_s^{H_\Omega} U_{t-s}^H)^\dagger A_X U_s^{H_\Omega} U_{t-s}^H \right\| \\ &\leq \int_0^{|t|} ds \left\| (U_{t-s}^H)^\dagger [H - H_\Omega, (U_s^{H_\Omega})^\dagger A_X U_s^{H_\Omega}] U_{t-s}^H \right\| \\ &\leq \int_0^{|t|} ds \sum_{Y:Y \sim \Omega^c} \| [A_X(s; H_\Omega), h_Y] \| \end{aligned} \quad (\text{A25})$$

(In the last inequality the sum over Y could be further restricted to those with $Y \sim \Omega$, but the present bound will be enough.) The last line can be bounded by multiplying (A17) by $2 \|B\| = 2 \|h_Y\|$ and summing over Y such that $Y \sim \Omega^c$. The innermost sum of (A17) is modified to

$$\begin{aligned} \sum_{Z_k: (Z_{k-2} \cup Z_{k-1}) \sim Z_k} \|h_{Z_k}\| \sum_{Y: Z_k \sim Y \sim \Omega^c} \|h_Y\| &\quad \text{if } k \text{ is odd,} \\ \sum_{Z_{k-1}, Z_k: (Z_{k-3} \cup Z_{k-2}) \sim Z_{k-1} \sim Z_k} \|h_{Z_{k-1}}\| \|h_{Z_k}\| \sum_{Y: Z_k \sim Y \sim \Omega^c} \|h_Y\| &\quad \text{if } k \text{ is even.} \end{aligned} \quad (\text{A26})$$

The sum over Y here is bounded by (A19), and the remaining sum is bounded by applying (A20) once or twice. The net effect of the modification is that there is an extra factor of ζ , and that the distance is now measured to Ω^c instead of Y before. We conclude that

$$\|A_X(t; H) - A_X(t; H_\Omega)\| \leq \frac{2\zeta|t|}{\sqrt{\eta}} \|A\| \left(\exp\left(\zeta|t|\sqrt{8\eta}\right) - 1 \right) \sum_{x \in X} \exp(-\mu \text{ dist}(x, \Omega^c)). \quad (\text{A27})$$

Since $\eta \leq 2$, this proves a variant of Lemma 3 where the locality assumption is given by (A2).

In Lemma 3 we assumed strictly local interactions such that $h_X = 0$ if $\text{diam}(X) > 1$ in a D -dimensional lattice. This strict locality condition implies (A2) with arbitrary $\mu > 0$ (ζ can be estimated as a function of μ), and hence the bound is sufficient for Theorem 1. However, one can prove a stronger bound for the strictly local interactions. Since $D_B(X, t) \leq \|h_X\| C_B(X, t)$, we have

$$C_B(X, t) \leq C_B(X, 0) + 2 \sum_{Z: X \sim Z} \|h_Z\| \int_0^{|t|} ds C_B(Z, s) \quad (\text{A28})$$

$$\leq 2 \|B\| \sum_{k=1}^{\infty} \frac{(2|t|)^k}{k!} \sum_{Z_1, \dots, Z_k: \text{linked}} \prod_{j=1}^k \|h_{Z_j}\| \quad (\text{A29})$$

where ‘‘linked’’ means that $X \sim Z_1 \sim Z_2 \sim \dots \sim Z_k \sim Y$. Similarly to Proposition 13, we see for

arbitrary sets P, Q, S of sites

$$\sum_{Q:P \sim Q \sim S} \|h_Q\| \leq \zeta_0 \sum_{p \in P} \delta_{\text{dist}(p, S) \leq 1}, \quad (\text{A30})$$

$$\sum_{Q:P \sim Q} |Q| \|h_Q\| \delta_{\text{dist}(Q, S) \leq d} \leq \zeta_0 \sum_{p \in P} \delta_{\text{dist}(p, S) \leq d+1} \quad (\text{A31})$$

where $\zeta_0 = \max_{x \in \Lambda} \sum_{Q \ni x} |Q| \|h_Q\|$. Note that ζ_0 is bounded by the number of nonzero Hamiltonian terms that may act on a site p , and the number of sites in a ball of diameter 1. We conclude that

$$C_B(X, t) \leq 2 \|B\| \sum_{x \in X} \sum_{k=\lfloor \text{dist}(x, Y) \rfloor}^{\infty} \frac{(2\zeta_0|t|)^k}{k!}, \quad (\text{A32})$$

$$\|[A_X(t), B_Y]\| \leq 2 \|A\| \|B\| |X| \frac{(2\zeta_0|t|)^\ell}{\ell!} e^{2\zeta_0|t|} \text{ where } \ell = \lfloor \text{dist}(X, Y) \rfloor \quad (\text{A33})$$

by Taylor's theorem applied to e^x . By analogous manipulation as above, we also have

$$\|A_X(t; H) - A_X(t; H_\Omega)\| \leq |X| \|A_X\| \frac{(2\zeta_0|t|)^\ell}{\ell!} e^{2\zeta_0|t|} \quad (\text{A34})$$

where $\ell = \lfloor \text{dist}(X, \Lambda \setminus \Omega) \rfloor$. This completes the proof of [Lemma 3](#).

5. Higher Order Commutators

Finally, let us remark that even better bounds can be proven if one assumes a bound on higher-order commutators. For example, if we assume that

$$\|[[h_X, h_Y], h_Z]\| \leq \eta' \|h_X\| \cdot \|h_Y\| \cdot \|h_Z\|, \quad (\text{A35})$$

we can prove a better bound for sufficiently small η' . This is done by an straightforward generalization of the above results: In addition to quantities $C_B(X, t)$ and $D_B(X, t)$, define also a quantity $E_B(X, Y, t)$ as

$$E_B(X, Y, t) = \|[[h_X(t), h_Y(t)], B]\|. \quad (\text{A36})$$

Then, just as we bound $C_B(X, t + dt) - C_B(X, t)$ in terms of $D_B(X, t)$ above, we also bound $D_B(X, t + dt) - D_B(X, t)$ in terms of $E_B(X, Y, t)$ summed over sets Y that intersect X . Then, we bound $E_B(X, Y, t + dt) - E_B(X, Y, t)$ using Eq. (A35). Extensions to even higher commutators follow similarly. For such higher order commutators, a natural assumption to replace Eq. (A2) is that

$$\sum_{X \ni x} \|h_X\| |X|^\beta \exp(\mu \text{ diam}(X)) \leq \zeta < \infty \quad (\text{A37})$$

where β is the order of the commutator that we bound (i.e, $\beta = 2$ for Eq. (A1), $\beta = 3$ for Eq. (A35), and so on).

Appendix B: Analytic functions are efficiently computable

Here we briefly review a polynomial approximation scheme to *analytic* functions — that have power series representations.³ For $\rho > 1$, define E_ρ to be the *Bernstein ellipse*, the image of a circle $\{z \in \mathbb{C} : |z| = \rho\}$ under the map $z \mapsto \frac{1}{2}(z + z^{-1})$. The Bernstein ellipse always encloses $[-1, 1]$, and as $\rho \rightarrow 1$, the Bernstein ellipse collapses to $[-1, 1] \subset \mathbb{C}$. It is useful to introduce *Chebyshev polynomials* (of the first kind) T_m of degree $m \geq 0$, defined by the equation

$$T_m\left(\frac{z + z^{-1}}{2}\right) = \frac{z^m + z^{-m}}{2}. \quad (\text{B1})$$

Picking z on the unit circle, we see that $T_m : [-1, 1] \ni \cos \theta \mapsto \cos m\theta \in [-1, 1]$. The leading coefficient of T_m has to be 2^{m-1} , as seen by comparing the leading term in Eq. (B1).

Lemma 14. *Let f be a analytic function on the interior of E_ρ for some $\rho > 1$, and assume $\sup_{z \in E_\rho} f(z) = M < \infty$. Then, f admits an approximate polynomial expansion in Chebyshev polynomials such that*

$$\max_{x \in [-1, 1]} \left| f(x) - \sum_{j=0}^J a_j T_j(x) \right| \leq \frac{2M}{\rho - 1} \rho^{-J}. \quad (\text{B2})$$

Proof. The series expansion is a disguised cosine series:

$$f(\cos \theta) = \sum_{j=0}^{\infty} a_j T_j(\cos \theta) = \sum_{j=0}^{\infty} a_j \cos(j\theta). \quad (\text{B3})$$

It is important that $\theta \mapsto f(\cos \theta)$ is a periodic smooth function, and therefore its Fourier series converges to the function value. The coefficients can be read off by

$$a_j = \frac{1}{\pi} \int_0^{2\pi} d\theta f(\cos \theta) \cos j\theta \quad (j > 0), \quad (\text{B4})$$

$$a_0 = \frac{1}{2\pi} \int_0^{2\pi} d\theta f(\cos \theta) \quad (j = 0). \quad (\text{B5})$$

The assumption on the analyticity means that $z \mapsto f(\frac{1}{2}(z + z^{-1}))$ is analytic on the annulus $\{z \in \mathbb{C} : \rho^{-1} < |z| < \rho\}$. Thus, we can write the above integral as a contour integral along the

³ An example of smooth but non-analytic function is $\exp(-z^{-2})$. This function fails to be analytic at $z = 0$. It is infinitely differentiable at $z = 0$, with derivatives all zero, and hence the Taylor series is identically zero, but the function is not identically zero around $z = 0$. If a real function is analytic at $x \in \mathbb{R}$, then its power series converges in an open neighborhood of x in the complex plane (analytic continuation).

circle $C_\rho = \{z \in \mathbb{C} : |z| = \rho\}$, and obtain a bound for $j > 0$

$$\begin{aligned} |a_j| &= \left| \frac{1}{i\pi} \int_{C_\rho} \frac{dz}{z} f\left(\frac{z+z^{-1}}{2}\right) \frac{z^j + z^{-j}}{2} \right| \\ &= \frac{1}{\pi} \left| \int_{C_\rho} f\left(\frac{z+z^{-1}}{2}\right) z^{-j-1} \right| \\ &\leq \frac{2M}{\rho^j} \end{aligned} \quad (\text{B6})$$

where the second equality is due to the symmetry $z \leftrightarrow z^{-1}$ of the integrand. For $j = 0$, we know $|a_0| \leq M$. Since $|T_j(x)| \leq 1$ for $x \in [-1, 1]$, this completes the proof. \square

Therefore, a function on $[-1, 1]$ that is analytic over E_ρ can be computed to accuracy ϵ by evaluating a polynomial of degree $\mathcal{O}(\log(1/\epsilon))$.

Appendix C: Hamiltonian simulation by quantum signal processing and Qubitization

In this section, we outline Hamiltonian simulation of e^{-itH} by quantum signal processing [4] and Qubitization [5] in three steps, and introduce a simple situational circuit optimization for constant factor improvements in gate costs.

First, one assumes that the Hamiltonian H acting on register s is encoded in a certain standard-form:

$$(\langle G|_a \otimes \mathbf{1}_s)O(|G\rangle_a \otimes \mathbf{1}_s) = H/\alpha. \quad (\text{C1})$$

Here, we assume access to a unitary oracle O that acts jointly on registers a, s , and a unitary oracle G that prepares some state $G|0\rangle_a = |G\rangle_a$ such that Eq. (C1) is satisfied with some normalization constant $\alpha \geq \|H\|$. Note that α represents the quality of the encoding; a smaller α leads fewer overall queries to O and G .

Second, the Qubitization algorithm queries \hat{O} and G to construct a unitary W , the qubiterate, with eigenphases $\phi_\lambda = \sin^{-1}(\lambda/\alpha)$ directly related to eigenvalues of the Hamiltonian $H|\lambda\rangle = \lambda|\lambda\rangle$. In the case where $\hat{O}^2 = \mathbf{1}_{as}$, this is accomplished by a reflection about $|G\rangle_a$:

$$W = -i((2|G\rangle\langle G|_a - \mathbf{1}_a) \otimes \mathbf{1}_s) \hat{O}. \quad (\text{C2})$$

For every eigenstate $|\lambda\rangle$, the normalized states

$$\begin{aligned} |G_\lambda\rangle &= |G\rangle_a |\lambda\rangle_s, & |G_\lambda^\perp\rangle &\propto (1 - \langle G_\lambda| W |G_\lambda\rangle) |G_\lambda\rangle, \\ |G_{\lambda\pm}\rangle &= \frac{1}{\sqrt{2}}(|G_\lambda\rangle \pm i|G_\lambda\rangle) \end{aligned} \quad (\text{C3})$$

are eigenstate of W with eigenvalues

$$W|G_{\lambda\pm}\rangle = \mp e^{\pm i\phi_\lambda} |G_{\lambda\pm}\rangle, \quad \phi_\lambda = \sin^{-1}(\lambda/\alpha). \quad (\text{C4})$$

Third, the quantum signal processing algorithm queries the qubiterate to approximate a unitary V which has the same eigenstates $|G_{\lambda\pm}\rangle$, but with eigenphases transformed like $\mp e^{\pm i\phi_\lambda} \rightarrow e^{-i\alpha t \sin(\phi_\lambda)} = e^{-it\lambda}$. As this applies the same phase regardless of the \pm sign, time evolution by e^{-itH} is accomplished as follows:

$$\begin{aligned} V|G_\lambda\rangle &= V \frac{|G_{\lambda+}\rangle + |G_{\lambda-}\rangle}{\sqrt{2}} = V \frac{e^{-it\lambda}|G_{\lambda+}\rangle + e^{-it\lambda}|G_{\lambda-}\rangle}{\sqrt{2}} = e^{-it\lambda}|G\rangle_a|G_\lambda\rangle \\ &\Rightarrow (\langle G|_a \otimes \mathbf{1}_s)V(\langle G\rangle_a \otimes \mathbf{1}_s) = e^{-itH}. \end{aligned} \quad (\text{C5})$$

Quantum signal processing here is accomplished by a unitary sequence $V_{\vec{\varphi}}$ of controlled- W interspersed by single-qubit operations, parameterized by $\vec{\varphi} \in \mathbb{R}^N$, on the single-qubit ancilla register b , defined as follows:

$$\begin{aligned} V_{\vec{\varphi}} &= V_{\pi+\varphi_N}^\dagger V_{\varphi_{N-1}}^\dagger V_{\pi+\varphi_{N-2}}^\dagger V_{\varphi_{N-3}} \cdots V_{\pi+\varphi_2}^\dagger V_{\varphi_1}, \\ V_\varphi &= (e^{-i\varphi Z/2} \text{Hd} \otimes I_{as})(|0\rangle\langle 0|_b \otimes I_{as} + |1\rangle\langle 1|_b \otimes W)(\text{Hd} e^{i\varphi Z/2} \otimes I_{as}), \end{aligned} \quad (\text{C6})$$

where Hd is the Hadamard gate. For every eigenstate $W|\nu\rangle_{as} = e^{i\phi_\nu}|\nu\rangle_{as}$, the controlled operator $V_{\vec{\varphi}}$ acting on $|\nu\rangle_{as}$ introduces a phase kickback ϕ_ν on the ancilla register b . This phase is transformed by the similarity operation

$$e^{i\phi/2}e^{-i\varphi Z/2} \text{Hd} e^{-i\varphi Z/2} \text{Hd} e^{i\varphi Z/2} = e^{i\phi/2}e^{-i\phi P_\varphi/2}, \quad P_\varphi = \cos(\varphi)X + \sin(\varphi)Y. \quad (\text{C7})$$

Thus by multiplying out the single qubit-rotations,

$$\begin{aligned} (\langle +|_b \langle \nu|_{as})V_{\vec{\varphi}}(|+\rangle_b |\nu\rangle_{as}) &= \langle +|_b e^{-i\phi_\nu P_{\varphi_N}/2} e^{-i\phi_\nu P_{\varphi_{N-1}}/2} \cdots e^{-i\phi_\nu P_{\varphi_1}/2} |+\rangle_b \\ &= \langle +|_b \sum_{k=0}^{N/2} (a_k I + i b_k Z) \cos(k\phi_\nu) + i(c_k X + d_k Y) \sin(k\phi_\nu) |+\rangle_b, \\ &= \sum_{k=0}^{N/2} a_k \cos(k\phi_\nu) + i c_k \sin(k\phi_\nu), \end{aligned} \quad (\text{C8})$$

where the $\{a, b, c, d\}$ are real coefficients.

The desired phase transformation $\mp e^{\pm i\phi_\lambda} \rightarrow e^{-i\alpha t \sin(\phi_\lambda)}$ may then be approximated by choosing the coefficients $\{a, c\}$ to be the Bessel function coefficients $J_k(\alpha t)$ of the Jacobi-Anger expansion up to $k = N/2$.

$$e^{-i\alpha t \sin(\phi)} = \left(J_0(\alpha t) + 2 \sum_{k \text{ even } > 0}^{\infty} J_k(\alpha t) \cos(k\phi) \right) - i \left(2 \sum_{\text{odd } > 0}^{\infty} J_k(\alpha t) \sin(k\phi) \right) \quad (\text{C9})$$

Note that truncation error of this approximation is $\epsilon_{Trunc} \leq 2 \sum_{k=q}^{\infty} |J_k(\alpha t)|$. In principle, the angles $\vec{\varphi}$ that approximate the desired coefficients $\{a, c\}$ may be precomputed by a classical polynomial-time algorithm [23]. This ultimately leads to an approximation of $e^{-i\alpha t \sin(\phi)}$ with error

$$\epsilon_{\square} = \|(\langle +|_b \langle G|_a \otimes \mathbf{1}_s) V_{\vec{\varphi}} (|+\rangle_b |G\rangle_a \otimes \mathbf{1}_s) - e^{-itH}\| \leq 16 \sum_{k=q}^{\infty} |J_k(\alpha t)| \leq \frac{32(\alpha t)^q}{2^q q!}, \quad q = N/2 + 1. \quad (\text{C10})$$

When evaluating gate counts of this simulation algorithm, we will use placeholder values for $\vec{\varphi}$.

1. Encoding coefficients in reflections

With these three steps, the remaining challenge is explicitly constructing the oracles O and G that encode the desired Hamiltonian. For a general Hamiltonian represented as a linear combination of M Pauli operators P_j

$$H = \sum_{j=0}^{M-1} \alpha_j P_j, \quad \alpha_j > 0, \quad \alpha = \sum_{j=0}^{M-1} \alpha_j \quad (\text{C11})$$

The most straightforward approach defines

$$O = \sum_{j=0}^{M-1} |j\rangle \langle j| \otimes P_j, \quad |G\rangle_a = \sum_{j=0}^{M-1} \sqrt{\frac{\alpha_j}{\alpha}} |j\rangle_a. \quad (\text{C12})$$

It is easy to verify that $(\langle G|_a \otimes \mathbf{1}_s) O (|G\rangle_a \otimes \mathbf{1}_s) = H/\alpha$, and $O^2 = \mathbf{1}_{as}$, as desired. The gate complexity O and G are asymptotically similar: The control logic for O may be constructed using $\mathcal{O}(M)$ NOT, CNOT, and Toffoli gates [2], and the creation of an arbitrary dimension M quantum state requires $\mathcal{O}(M)$ CNOT, Hadamard, T, and arbitrary single-qubit phase rotations $e^{i\phi Z}$ [24].

However, if many coefficients α_j of H are identical, the use of arbitrary state preparation is excessively costly. For instance, in the extreme case where all α_j are identical, and M is a power of 2, $\log_2 M$ Hadamard gates suffice to prepare $|G\rangle_a$ – when M is not a power of two, a uniform superposition over all states up to M may still be prepared with cost $\mathcal{O}(\log M)$ by combining integer arithmetic with amplitude amplification. In another case where only a few α_j differ, one may exploit a unary representation of the control logic [25] to accelerate the preparation of $|G\rangle$ at the cost of additional space overhead.

Rather than encoding coefficient information in the state $|G\rangle$, one simple alternate approach is to encode coefficient information by replacing the operators P_j with exponentials $U_j = e^{-iP_j \cos^{-1}(\alpha_j)}$ by taking a linear combination of $\frac{U_j + U_j^\dagger}{2} = \alpha_j P_j$. However, as $U_j^2 \neq \mathbf{1}$ in general, the downside of

this approach is that $O^2 \neq \mathbf{1}_{as}$, which negates the prerequisite for the simple qubitization circuit of Eq. (C2).

We present a simple modification that allows us to encode coefficient information in unitary operators whilst maintaining the condition $O^2 = \mathbf{1}_{as}$. Consider the two-qubit circuit acting on register c .

$$Q_j = (I \otimes e^{i\beta_j X}) \text{SWAP}(I \otimes e^{-i\beta_j X}), \quad Q_j^2 = I_{12}, \quad \langle 00 | Q_j | 00 \rangle = \cos^2(\beta_j) \quad (\text{C13})$$

where $\beta_j > 0$. Thus if we define

$$O = \sum_{j=0}^{M-1} |j\rangle\langle j| \otimes Q_j \otimes P_j, \quad |G\rangle_{ac} = \sum_{j=0}^{M-1} \frac{1}{\sqrt{M}} |j\rangle_a |00\rangle_c, \quad (\text{C14})$$

then $O^2 = \mathbf{1}_{abc}$ and this encodes the Hamiltonian

$$(\langle G |_{ac} \otimes \mathbf{1}_s) O (|G\rangle_{ac} \otimes \mathbf{1}_s) = \frac{1}{M} \sum_{j=0}^{M-1} \cos^2(\beta_j) P_j. \quad (\text{C15})$$

This construction is advantageous in the situation, such as in Eq. (6) where most coefficients are 1, and only a few are less than one – whenever $\beta_j = 0$, we replace Q_j with the identity operator.

- [1] Julia Kempe, Alexei Kitaev, and Oded Regev, “The complexity of the local Hamiltonian problem,” *SIAM Journal on Computing* **35**, 1070–1097 (2006), [quant-ph/0406180](#).
- [2] Andrew M. Childs, Dmitri Maslov, Yunseong Nam, Neil J. Ross, and Yuan Su, “Toward the first quantum simulation with quantum speedup,” [1711.10980v1](#).
- [3] Dominic W. Berry, Andrew M. Childs, Richard Cleve, Robin Kothari, and Rolando D. Somma, “Simulating Hamiltonian dynamics with a truncated Taylor series,” *Phys. Rev. Lett.* **114**, 090502 (2015), [1412.4687](#).
- [4] Guang Hao Low and Isaac L. Chuang, “Optimal Hamiltonian simulation by quantum signal processing,” *Phys. Rev. Lett.* **118**, 010501 (2017), [1606.02685v2](#).
- [5] Guang Hao Low and Isaac L Chuang, “Hamiltonian simulation by qubitization,” (2016), [1610.06546](#).
- [6] H. F. Trotter, “On the product of semi-groups of operators,” *Proceedings of the American Mathematical Society* **10**, 545–545 (1959).
- [7] Masuo Suzuki, “General theory of fractal path integrals with applications to many-body theories and statistical physics,” *Journal of Mathematical Physics* **32**, 400–407 (1991).
- [8] Elliott H. Lieb and Derek W. Robinson, “The finite group velocity of quantum spin systems,” *Communications in Mathematical Physics* **28**, 251–257 (1972).
- [9] M. B. Hastings, “Lieb-Schultz-Mattis in higher dimensions,” *Phys. Rev. B* **69**, 104431 (2004), [cond-mat/0305505](#).

- [10] Bruno Nachtergaae and Robert Sims, “Lieb-Robinson bounds and the exponential clustering theorem,” *Commun. Math. Phys.* **265**, 119–130 (2006), [math-ph/0506030v3](#).
- [11] Matthew B. Hastings and Tohru Koma, “Spectral gap and exponential decay of correlations,” *Commun. Math. Phys.* **265**, 781–804 (2006), [math-ph/0507008](#).
- [12] M. B. Hastings, “Locality in quantum systems,” (2010), [1008.5137](#).
- [13] Tobias J. Osborne, “The dynamics of 1D quantum spin systems can be approximated efficiently,” *Phys. Rev. Lett.* **97**, 157202 (2006), [quant-ph/0508031](#).
- [14] Spyridon Michalakis, “Stability of the area law for the entropy of entanglement,” [1206.6900](#).
- [15] Dominic W. Berry, Andrew M. Childs, Richard Cleve, Robin Kothari, and Rolando D. Somma, “Exponential improvement in precision for simulating sparse Hamiltonians,” (2014) pp. 283–292, [1312.1414](#).
- [16] D. W. Berry, A. M. Childs, and R. Kothari, “Hamiltonian simulation with nearly optimal dependence on all parameters,” in *2015 IEEE 56th Annual Symposium on Foundations of Computer Science* (2015) pp. 792–809, [1501.01715](#).
- [17] A. Yu. Kitaev, A. H. Shen, and M. N. Vyalyi, *Classical and Quantum Computation*, Vol. GSM 47 (American Mathematical Society, 2002).
- [18] Dominic W. Berry, Graeme Ahokas, Richard Cleve, and Barry C. Sanders, “Efficient quantum algorithms for simulating sparse Hamiltonians,” *Communications in Mathematical Physics* **270**, 359–371 (2007), [quant-ph/0508139](#).
- [19] Adriano Barenco, Charles H. Bennett, Richard Cleve, David P. DiVincenzo, Norman Margolus, Peter Shor, Tycho Sleator, John A. Smolin, and Harald Weinfurter, “Elementary gates for quantum computation,” *Phys. Rev. A* **52**, 3457–3467 (1995), [quant-ph/9503016](#).
- [20] Emanuel Knill, “Approximation by quantum circuits,” (1995), [quant-ph/9508006](#).
- [21] Michael A. Nielsen and Isaac L. Chuang, *Quantum Computation and Quantum Information* (Cambridge University Press, 2000).
- [22] Stanislaw J. Szarek, “Metric entropy of homogeneous spaces and finsler geometry of classical lie groups,” (1997), [math/9701204](#).
- [23] Guang Hao Low, Theodore J. Yoder, and Isaac L. Chuang, “Methodology of resonant equiangular composite quantum gates,” *Phys. Rev. X* **6**, 041067 (2016), [1603.03996](#).
- [24] Vivek V Shende, Stephen S Bullock, and Igor L Markov, “Synthesis of quantum-logic circuits,” *IEEE Transactions on Computer-Aided Design of Integrated Circuits and Systems* **25**, 1000–1010 (2006), [quant-ph/0406176](#).
- [25] David Poulin, Alexei Kitaev, Damian S Steiger, Matthew B Hastings, and Matthias Troyer, “Fast quantum algorithm for spectral properties,” (2017), [1711.11025](#).